Risk analysis in road tunnels – a metamodel to efficiently integrate complex fire scenarios

Florian Berchtold[1], Christian Knaust[1], Lukas Arnold[2], Sebastian Thöns[3] & Andreas Rogge[1]
[1]Bundesanstalt für Materialforschung und Prüfung (BAM), Berlin, Germany
[2]Forschungszentrum Jülich, Jülich, Germany
[3]Technical University of Denmark (DTU), Lyngby, Denmark

ABSTRACT
Fires in road tunnels constitute complex scenarios, described by risk indicators, including possible interactions between the fire, tunnel users and safety measures. More and more methodologies for risk analysis quantify consequences of complex scenarios with complex consequence models. An example for a complex consequence model is the computational fluid dynamics coupled with microscopic evacuation model Fire Dynamics Simulator (FDS) with FDS+Evac. However, the high computational effort of complex consequence models often limits the number of scenarios in practice, which leads to simplifications in the scenarios. Accordingly, there is a challenge to consider complex scenarios in risk analysis.
To face this challenge, we improved the metamodel used in the methodology for risk analysis presented on ISTSS 2016. Now, the metamodel consists of the projection array-based design, the moving least squares method, and the prediction interval to quantify the metamodel uncertainty. The metamodel quickly interpolates the consequences of few complex scenarios analysed with the complex consequence models to a large number of arbitrary scenarios. Additionally, we implemented two adaptions in the projection array-based design: first, the sequential refinement with focus on high metamodel uncertainties; and the combination of two designs for FDS and FDS+Evac.
In summary, we analyse the effects of three refinement steps on the metamodel and on the results of risk analysis. We observe convergence in both after the second step (ten scenarios in FDS, 192 scenarios in FDS+Evac) in comparison to ISTSS 2016 (20 scenarios in FDS, 800 evacuation scenarios). Thus, we reduced the number of scenarios remarkably with the improved metamodel.
In conclusion, we can now efficiently integrate complex scenarios in risk analysis. We further emphasise that the metamodel is broadly applicable on various experimental or modelling issues in fire safety engineering.

KEYWORD: risk, tunnel, fire, evacuation, CFD, metamodel, uncertainty, adaptivity

NOMENCLATURE

Roman and Greek letters

d	number of risk indicators (dimensions) in $\vec{x}$
$fa = [\overline{FA}, FA]$	failure of tunnel alarm [no, yes]
HRR_{max}	maximum heat release rate /MW
N_{tu}	number of tunnel users
n	number of scenarios
$p_{stretch}$	stretching factor
$q_{90}(\boldsymbol{s})$	90% quantile of $\boldsymbol{s}$
$s^2(\xi)$	variance of ξ
$\boldsymbol{s} = \boldsymbol{s}(\boldsymbol{\xi})$	vector of the root of variances of $\boldsymbol{\xi}$
$\tilde{t}_\alpha$	random realisation of the Student's t-distribution
$t_{crit,\alpha}$	critical value of the Student's t-distribution
t_{max}	time to maximum heat release rate /s

t_{pre}	maximum pre-evacuation time /s
$\vec{x}$	scenario
$\tilde{x}$	arbitrary (evacuation) scenario
X	experimental design for scenarios
α	two-sided confidence interval
$\boldsymbol{\Delta\xi}$	vector of the prediction interval
$\boldsymbol{\Delta\tilde{\xi}}$	vector of metamodel uncertainty
$\boldsymbol{\xi} = \boldsymbol{\xi}(\tilde{X})$	metamodel for the fraction of fatalities in arbitrary scenarios $\tilde{X}$
$\tilde{\boldsymbol{\xi}} = \tilde{\boldsymbol{\xi}}(\tilde{X})$	uncertain $\boldsymbol{\xi}$ with the metamodel uncertainty
$\boldsymbol{\xi^c} = \boldsymbol{\xi^c}(X^e)$	vector of fraction of fatalities (complex consequence model)

Superscripts and subscripts

c	complex consequence model
e	evacuation
f	fire
X	experimental design used as basis

INTRODUCTION

Fires in road tunnels constitute complex scenarios with interactions between the fire, tunnel users and safety measures like fire detection, tunnel alarm or emergency ventilation. Thus, many risk indicators, which are factors with effects on risks for tunnel users, describe the complex scenario. Several methodologies for risk analysis in road tunnels evolved during the last 15 years [1] to determine the risks and to evaluate the effects of safety measures. To take the complex scenarios into account, more and more of these methodologies now apply complex consequence models to quantify the consequences. The complex consequence models can consist of two parts: first, fire models like computational fluid dynamics models which simulate the spread of heat and smoke in a fire scenario; and second, microscopic evacuation models which simulate the movement of individual tunnel users as well as their interactions in an evacuation scenario. But complex consequence models cause high computational effort what often strongly limits the number of scenarios in practical applications. Furthermore, risk analysis requires consequences of an 'infinite' number of scenarios on the entire domain of risk indicators, e.g. from low to high heat release rates. Thus, risk analysis pursues a 'global objective' instead of focusing on interesting regions of the domain, e.g. only on high heat release rates (local objective) [2]. Together with the high computational effort, the global objective limits the number of risk indicators leading to reduced complexity of scenarios, e.g. in [3]. Concluding, there is a challenge for risk analysis to integrate complex scenarios considering several risk indicators with complex consequence models.

To face this challenge, we improved the metamodel used in our methodology for risk analysis published on ISTSS 2016 [4]. In general, a metamodel consists of two parts [5]. First, the experimental design defines the parameters of risk indicators for a small number of scenarios. Then, the consequences of these scenarios will be quantified with the complex consequence model and saved in a permanent data base. Second, the response surface model, interpolates the consequences from the data base to any arbitrary scenario. The interpolation is very quick allowing the analysis of 'infinite' scenarios on the entire domain but causes uncertainties called metamodel uncertainty. Different models for both parts of the metamodel exist. First, several experimental designs address global objectives with good space-filling properties. Space-filling means an even spread of a small number of scenarios on the entire domain. For this purpose, Latin hypercube designs are very common [5], in particular with some optimisations in space-filling [6]. But the projection array-based design [7] improves the space-filling properties of Latin Hypercube designs in particular for high-dimensional problems. Furthermore, it is possible to append new scenarios to an existing projection array-based design in sequential refinement steps. Second, first- or second-order models are typical response surface models often used for local objectives [5]. Instead, the moving least squares method focuses on the global objective [8]. Thus, it allows an accurate interpolation on the entire domain. Additionally, the prediction interval [9] quantifies the metamodel uncertainties of the moving least

squares method. In brief, we adapted the models for both parts correspondingly in order to improve the metamodel.
Consequently, this paper outlines the metamodel in Section 'Methodology' and Section 'Results and discussion' focuses on proofing its efficiency. In detail, we organised the paper as follows. Section 'Methodology' consists of four subsections. First, 'Risk analysis with complex consequence models' describes the complex scenario, the risk indicators [4] and the computational fluid dynamics model Fire Dynamics Simulator FDS [10] and the microscopic evacuation model FDS+Evac [11]. Second, 'Experimental design' deals with the projection array-based design [7]. We also outline our adaptions: the focus on particular regions of the domain during sequential refinement; and the combination of two experimental designs for FDS and FDS+Evac. Third, 'Response Surface Model' provides the background to the moving least squares method [8]. The subsection also addresses our implementation of the metamodel uncertainty based on the prediction interval [9]. And fourth, 'Setup of the metamodel' shortly summarises the setup of the metamodel and outlines the optimisation of the moving least squares models. Then, Section 'Results and discussion' shows the different refinement steps. The Subsection 'Metamodel' highlights their effects on the moving least squares model and the metamodel uncertainty. The Subsection 'Risk analysis' shows the effects on risk measures and discusses the advantages to the metamodel used in ISTSS 2016 [4]. Finally, Section 'Conclusions' concludes that first, the metamodel efficiently integrates complex scenarios and second, emphasises that the metamodel is not only limited to risk analysis but also applicable on various issues in fire safety engineering.

METHODOLOGY

We put the focus of this paper on the improved metamodel, which is now used within the same methodology for risk analysis presented in [4]. Thus, we only provide the essential information of the methodology for risk analysis in the first Subsection and refer to [4] for further information. Then, Subsections 'Experimental design' and 'Response surface model' describe in detail the first and second part of the metamodel. Finally, we summarise how to setup the metamodel in Subsection 'Setup of the metamodel'.

Risk analysis with complex consequence models

The methodology for risk analysis [4] comprises twelve risk indicators, which define the scenario as well as the initial frequency of the fire. Risk indicators are factors affecting the risks in the road tunnel and rely on probabilistic, empirical or analytical models. We chose the risk indicators based on a literature review described in [4,12] and quantified the results of risk analysis with the two risk measures [13]: first, the individual risk R_{ind} is the annual frequency that a person being permanently in the tunnel will die due to a fire scenario; second, the societal risk, often presented in societal risk curves, is the annual frequency that a specified minimum number of persons will die due to a fire scenario. In summary, the risk measures depend on the consequences and on the initial frequency of fire in an 'infinite' number of arbitrary scenarios.
In case of a fire, five risk indicators define the fire and the evacuation scenario $\vec{x}$ (see Table 1). Two of these risk indicators affect the spread of heat and smoke in the fire scenario $\vec{x}_i^f = [HRR_{max,i}, t_{max,i}]$. The evacuation scenario, the evacuation of tunnel users during the fire scenario, considers three additional risk indicators $\vec{x}_j^e = [\vec{x}_j^f, t_{pre,j}, N_{tu,j}, fa_j]$. The maximum pre-evacuation time t_{pre} is the maximum duration between the alarm of a tunnel user and the beginning of its movement. The individual pre-evacuation time of a tunnel user is governed by a uniform probability distribution between zero and t_{pre}. The risk indicators t_{max} and t_{pre} use uniform probability distributions because of scarce statistical basis (see Table 1). For the risk indicators HRR_{max} and N_{tu} the probability distributions are twofold: for the evaluation of the metamodel we apply uniform probability distributions (Table 1) and for risk analysis we use specific probability models (Table 2).

Table 1: risk indicators with uniform probability distribution (white background: fire scenario, grey background: evacuation scenario)

risk indicator	term	min	max	references / remark

maximum heat release rate	HRR_{max} /MW	25	200	[14]
time to maximum heat release rate	t_{max} /s	600	1200	[15,16]
maximum pre-evacuation time	t_{pre} /s	100	300	[17–19]
number of tunnel users	N_{tu}	30	180	30 vehicles in the evacuation area
failure of tunnel alarm	fa (Boolean)	no ($\overline{FA}$)	yes (FA)	$p(FA) = 0.01; p(\overline{FA}) = 0.99$ [20]

Table 2: risk indicators with specific probability models used for risk analysis (white background: fire scenario, grey background: evacuation scenario)

risk indicator	term	remark
maximum heat release rate	HRR_{max} /MW	discrete distribution from 5 MW to 100 MW according to [20]; assumption: no fatalities for $HRR_{max} < 25\ MW$
number of tunnel users	N_{tu}	depending on the numbers of vehicles and vehicle types according to [20]

The fire and evacuation scenarios include following interactions in the road tunnel shown in Figure 1. After the ignition, the heat release rate of the fire develops with an exponential curve with the risk indicators HRR_{max} and t_{max} [21]. Accordingly, heat and smoke spread within the tunnel. Following the fire detection triggered by the heat release rate, the longitudinal emergency ventilation begins and the tunnel alarm alerts all tunnel users at the same time ($\overline{FA}$). But in case of a failure of tunnel alarm (FA), each tunnel user individually gets alerted by smoke depending on its initial position in the evacuation area. A tunnel user starts to move towards the emergency exit after its alarm and its individual pre-evacuation time which is less than t_{pre}. Thereby, smoke can impede the individual movement speed and tunnel users might interact in particular close to the emergency exit or in scenarios with high number of tunnel users N_{tu}. A tunnel user accounts to the number of fatalities if its fractional effective dose reaches the fatal limit [11]. Finally, the evacuation scenario leads to the fraction of fatalities which is the number of fatalities per number of tunnel users N_{tu}.

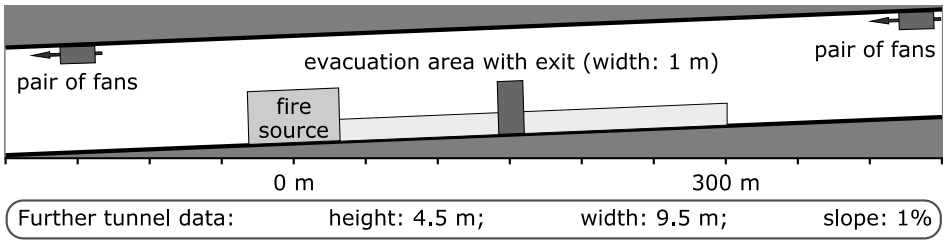

Figure 1 tunnel geometry of the scenario

We use the complex consequence model to determine the fraction of fatalities ξ^c in the fire and evacuation scenarios. The complex consequence model is a combination of the computational fluid dynamics model Fire Dynamics Simulator FDS [10] and the microscopic evacuation model FDS+Evac [11]. The fire model FDS simulates the spread of heat and smoke in the fire scenarios. The evacuation model FDS+Evac simulates the evacuation scenario and therefore adopts the spread of heat and smoke of a fire scenario simulated with FDS. FDS+Evac considers individual tunnel users with several random initial conditions like individual characteristics. To take the random initial conditions into account, we run 100 replications of one evacuation scenario. We then determine the mean fraction of fatalities ξ^c among these replications. Due to the high computational effort of FDS, we analyse less fire scenarios than evacuation scenarios with the complex consequence model. Thus, different evacuation scenarios consider the same fire scenario.

To conclude this Subsection, we built the definition of risk indicators and the scenario on an extended literature review [4,12]. The scenario covers the fire growth, important safety measures including the failure of tunnel alarm as well as the individual reaction and evacuation of tunnel users. But a vast number of further risk indicators is available, e.g. the fraction of tunnel users with physical disabilities. For this reason, the metamodel easily allows to include adapted scenarios depending on special applications in the methodology for risk analysis. But even without further adaptions, the scenario with five risk indicators in total is more complex compared to other common methodologies for risk analysis, e.g. [3].

Experimental design

The experimental design constitutes the first part of the metamodel and defines the set of n scenarios. We denote the experimental design in general with $X = [\vec{x}_1, \vec{x}_2, \dots, \vec{x}_n]^T$ with d risk indicators defining a scenario $\vec{x}_i$. Fire scenarios and evacuation scenarios depend on different risk indicators and thus have two separate experimental designs. The experimental designs for n_f fire scenarios and n_e evacuation scenarios are: $X^f = \left[\left[HRR_{max,i}, t_{max,i}\right], \dots\right]^T$ and $X^e = \left[\left[HRR_{max,i}, t_{max,i}, t_{pre,i}, N_{tu,i}\right], \dots\right]^T$. It has to be mentioned that X^e considers $d_e = 4$ risk indicators. The fifths risk indicator, the failure of tunnel alarm fa, is a Boolean and cannot be interpolated. Thus, the evacuation scenarios with $\overline{FA}$ and FA base on the same experimental design X^e. For the sake of simplicity, we use the same notation X^e for both cases and only specify the failure of tunnel alarm if required. Finally, FDS+Evac determines $\boldsymbol{\xi^c} = \boldsymbol{\xi_X^c} = [\xi_1^c, \dots, \xi_{n_e}^c]$ for $\overline{FA}$ and FA. We setup separate initial experimental design X_0 for the fire scenarios and the evacuation scenarios and then combine them with projection array-based designs [7] (see Figure 2). The initial experimental design has only scenarios at its corners which is the minimum requirement for the response surface model. We use the projection array-based design for its improved space-filling properties and the option for sequential refinement.

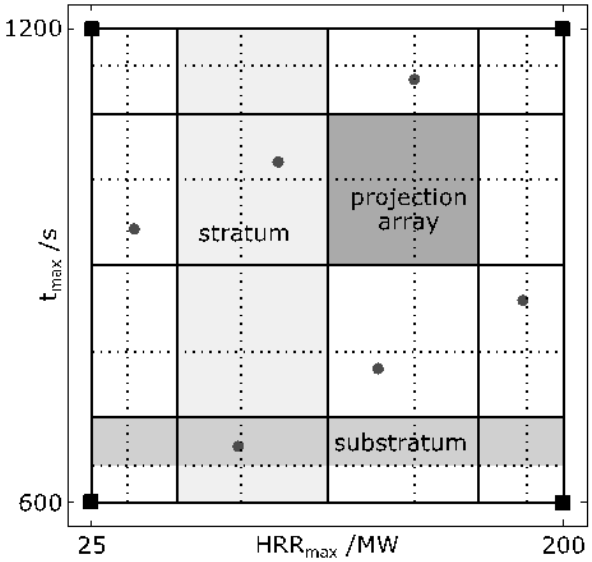

Figure 2 projection array-based design (circles) with the initial scenarios at the corners (squares). $p_{stretch} = 0.1$ with the underlying strata (solid lines) and substrata (dashed lines also behind the solid lines).

The projection array-based design extends the Latin hypercube design [22] with an additional underlying structure of projection arrays. The Latin hypercube design consists of n substrata in each dimension with exactly one scenario (lhd-condition). The projection arrays base on a fractional factorial design with $\left\lceil n^{\frac{1}{d}} \right\rceil$ number of strata in each dimension where $\lceil\ \rceil$ denotes the ceiling function. Hence, the number of projection arrays is always equal or higher than the number of scenarios n. The

projection array-based design demands maximum one scenario per projection array (pa-condition) as well as the lhd-condition. With regard to the lhd-condition we allow more than one scenario in a substratum for the initial experimental design. Therefore, all initial scenarios at the limits of each dimension count only as one scenario, e.g. leading to eight substrata for ten scenarios in Figure 2. For the sequential refinement of the projection array-based design, we augment the existing experimental design X_{i-1} with new scenarios X_{new} in sequential refinement steps: $X_i = \left[X_{i-1}^T, X_{new}^T\right]^T$. In conclusion, the pa-condition improves the space-filling properties compared to common Latin hypercube designs and thus meets the global objective of risk analysis.
We implemented two adaptions to the projection array-based design according to the requirements for risk analysis. First, to put focus on particular regions of the domain in each refinement step, we stretch the strata and substrata with the stretching parameter $p_{stretch}$, e.g. more to its centre with $p_{stretch} > 1$ or more to its boundaries with $p_{stretch} < 1$ (Figure 2). The procedure allows to maintain the pa- and lhd-condition. Second, we combine the fire and evacuation scenarios of the two separate experimental designs X^f and X^e to reduce the number of fire scenarios ($n_e > n_f$). For this, the evacuation scenario $\vec{x}_i^{e^*} \in X^{e^*}$ adopts parameters of a fire scenario $\vec{x}_j^f \in X^f$ leading to X^e with $\vec{x}_i^e = [\vec{x}_j^f, t_{pre,i}, N_{tu,i}, fa_i]$. Thus, different evacuation scenarios consider the same fire scenario which obviously leads to the loss of lhd-condition in $\vec{x}_j^f$ whereas the pa-condition is not affected. To sum up, the focus on particular regions of the domain and the combination of experimental designs can reduce the number of scenarios in the experimental designs.

Response surface model
In the second part of the metamodel, the response surface model nearly interpolates $\boldsymbol{\xi_X^c}$ for any arbitrary scenario $\tilde{x}$ to $\xi = \xi_X(\tilde{x})$. Therefore we use the moving least squares method [8] because it accounts for the global objective of risk analysis. The moving least squares method bases on a local weighted least squares fit of a linear or quadratic polynomial. The fit is local because of the distance-dependent weighting, based on a weighting function, of each $\xi_i^c \in \boldsymbol{\xi^c}$ to the local scenario $\tilde{x}$. Thus, there are other fits for different scenarios $\tilde{x}$ and hence the moving least squares method is more flexible than fits of one global polynomial. We apply linear polynomials for X^e with $n_e^{1/d_e} \leq 3$ and else quadratic polynomials in the moving least squares method. We furthermore implemented three different functions types each having one weighting parameter [9,23] for the weighting function. For this reason, the moving least squares method is adaptable to the different refinement steps. Finally, the metamodel can quickly interpolate the fraction of fatalities $\boldsymbol{\xi} = \boldsymbol{\xi_X} = \boldsymbol{\xi_X}(\tilde{X}^e)$ for many arbitrary scenarios $\tilde{X}^e$.
Obviously, the interpolation causes uncertainties called metamodel uncertainties. The metamodel uncertainty $\Delta\tilde{\xi} = |\xi - \xi^c|$ is the uncertain difference $\Delta\tilde{\xi}(\tilde{x})$ between $\xi(\tilde{x})$ to the unknown fraction of fatalities $\xi^c(\tilde{x})$ at any arbitrary scenario $\tilde{x} \notin X^e$. We use the prediction interval [9] to quantify the metamodel uncertainty. The prediction interval was developed 'for predicting the interval of "the value of a single future observation" at a point.' [9]. The prediction interval, denoted with $\Delta\xi$ (or the vector $\boldsymbol{\Delta\xi}$) is linear proportional to the root of the variance $s^2(\xi)$ (see equation 1).

$$\Delta\xi = \Delta\xi(\alpha) = t_{crit,\alpha} \cdot s(\xi) \tag{1}$$

The variance $s^2(\xi)$ underlies a Student's t-distribution with the two sided confidence interval α and $t_{crit,\alpha}$ as the critical value of the Student's t-distribution with $n_e - d_e$ degrees of freedom. We derive the following probabilistic metamodel uncertainty from the prediction interval: $\Delta\tilde{\xi} = \tilde{t}_\alpha \cdot s\,(\xi)$ (or $\boldsymbol{\Delta\tilde{\xi}}$) with $\tilde{t}_\alpha$ as random realisation of the Student's t-distribution from equation 1. As a result, the metamodel of the uncertain fraction of fatalities $\tilde{\xi}$ (or $\tilde{\boldsymbol{\xi}}$) is given in equation 2.

$$\tilde{\xi} = \xi + \Delta\tilde{\xi} = \xi + \tilde{t}_\alpha \cdot s(\xi) \tag{2}$$

Setup of the metamodel
To sum up, we used the following procedure to setup a metamodel. First, we build the experimental

designs X_i^f and X_i^e (Subsection 'Experimental design'). Second, we run simulations with the complex consequence models to yield $\boldsymbol{\xi}_{X_i}^{\boldsymbol{c}}$. Third, we optimise the weighting function of moving least squares method to $\boldsymbol{\xi}_{X_i}^{\boldsymbol{c}}$. The aim of the optimisation is to reduce the 90% quantile $q_{90}(\boldsymbol{s})$ of the variance with $\boldsymbol{s} = \boldsymbol{s}(\boldsymbol{\xi}) = [s(\xi(\vec{x}_i^e)), \dots]$ for scenarios $\vec{x}_i^e$ evenly distributed on the entire domain. As result of the optimisation, the response surface model of the metamodel uses one of the three function types with the weighting parameter. Finally, we used the metamodel for two purposes in the Section 'Results and discussion': first, to evaluate the effects of refinement steps on the metamodel and to define $p_{stretch}$ for the subsequent refinement step (Subsection 'Metamodel'); second, to determine $\tilde{\boldsymbol{\xi}}$ of arbitrary scenarios $\tilde{X}$ for the use in risk analysis (Subsection 'Risk analysis').

RESULTS AND DISCUSSION

In a first step, we setup two separate initial experimental designs X_0^f and X_0^e to analyse the effects of the refinement steps on the metamodel as well as on the risk analysis. Subsequently, we ran three additional refinement steps i with the procedure described in Subsection 'Setup of the metamodel' of Section 'Methodology' with the parameters shown in Table 3. For each experimental design X_i^e, we found the highest values of the variance $s^2(\xi)$ at the corners and boundaries of the domains. Accordingly, we focused the refinement steps for X_2 and X_3 on these regions with $p_{stretch} < 1.0$. As a result, we yielded the experimental designs shown in Figure 3. Finally, we now analyse the effects of the refinement steps on: first, the metamodel (Subsection 'Metamodel') using risk indicators shown in Table 1; second, results of risk analysis (Subsection 'Risk analysis') with risk indicators from Table 2.

Table 3: overview on the sequential refinement steps

refinement step	n_f,	n_e	$p_{stretch}$	$q_{90}(\boldsymbol{s}\,\vert\overline{FA})$	$q_{90}(\boldsymbol{s}\vert FA)$
X_0	4	16	---	0.157	0.147
X_1	6	48	1.0	0.059	0.052
X_2	10	96	0.1	0.029	0.029
X_3	14	144	0.01	0.028	0.035

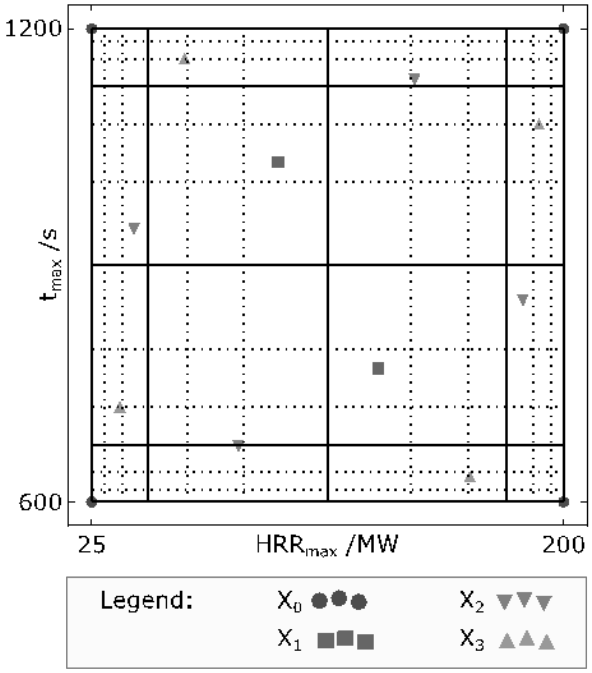

Figure 3 fire scenarios of all sequential refinement steps with the underlying strata (solid lines) and substrata (dashed lines) for X_3 with $p_{stretch} = 0.01$.

Metamodel

Table 3 shows the global effects of refinement steps on the variance $\boldsymbol{s}(\xi)$ with $q_{90}(\boldsymbol{s})$. The variance steadily decreased until refinement step X_2. The result of refinement step X_3 were twofold: for no failure of tunnel alarm ($\overline{FA}$) the variance was nearly constant but for failure of tunnel alarm (FA) the variance even increased. Thus, the refinement step X_2 lead to minimum variance with $n_e^{1/d_e} < 3.2$ evacuation scenarios along one dimension. Due to the combination of the experimental designs we required only ten fire scenarios instead of 96 for each evacuation scenario. In conclusion, the sequential refinement focussing on regions of the domain together with the combination of two experimental designs can lead to small numbers of simulations with the complex consequence models and hence reduces the computational effort.

The refinement steps had also local effects on the variance $s^2(\xi)$. Exemplarily, Figure 4 shows the variance of the refinement steps X_1 and X_2 for evacuation scenarios with $t_{pre} = 124\ s$ and $n_{tu} = 48$ with no failure of tunnel alarm. Refinement step X_1 had increased variances in the centre of the domain. With four new fire scenarios and 48 new evacuation scenarios, refinement step X_2 clearly decreased the variance in this region. From this result, we draw two conclusions: first, no additional scenarios were required in the centre of the domain; second, the sequential refinement with focus regions with high metamodel uncertainty can lead to an efficient decrease of the metamodel uncertainty.

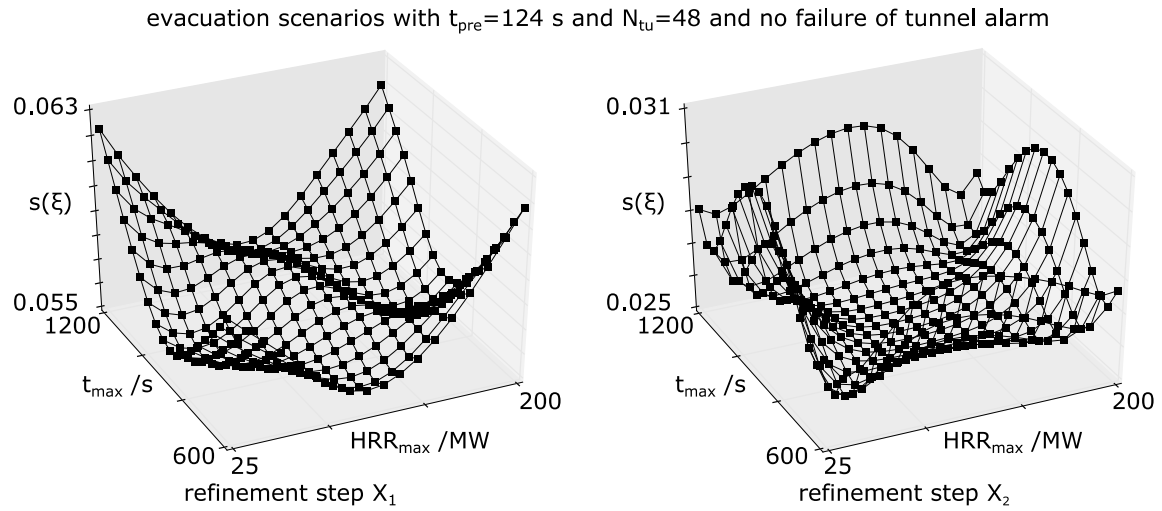

Figure 4 *root of the variance $\boldsymbol{s}(\xi)$ for X_1 (left) and X_2 (right). The increased variance in the centre vanishes after the refinement step.*

The moving least squares models $\boldsymbol{\xi}_{\boldsymbol{X_2}}$ and $\boldsymbol{\xi}_{\boldsymbol{X_3}}$ shown in Figure 5 strongly resemble global fits according to their quadratic polynomials. We found that the weighting function optimised with $q_{90}(\boldsymbol{s})$ lead to nearly global polynomial fits with only little distance-dependent weighting. This could be a possible reason for the increasing variance between X_2 and X_3 with failure of alarm shown in Table 3: the moving least squares model $\boldsymbol{\xi}$ did not adjust to new scenarios but stuck to the predefined global model of the quadratic polynomial. Or in other words: 'the response surface model is governed by the model instead of being governed by the response surface'. To cope with this drawback, the optimisation of the weighting function could focus on another measure leading to stronger distance dependent weighting but perhaps also to higher metamodel uncertainties.

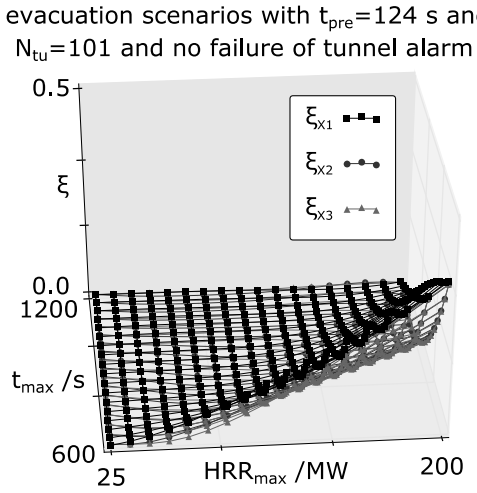

Figure 5 moving least squares models $\boldsymbol{\xi_{X_1}}$, $\boldsymbol{\xi_{X_2}}$, $\boldsymbol{\xi_{X_3}}$

To sum up, $\boldsymbol{\xi_{X_2}}$ and $\boldsymbol{\xi_{X_3}}$ resemble global polynomial fits. But in particular with regard to the local effects of refinement steps, we conclude that the metamodel $\boldsymbol{\xi_{X_2}}$ is close to the fraction of fatalities determined with the complex consequence models. For this reason, we apply the metamodel on risk analysis in the next Subsection.

Risk analysis

Subsequently, we analysed the effects of the experimental designs X_0, X_1, X_2, X_3 on the risk measures. Therefore, we ran a risk analysis with 10^6 random scenarios $\widetilde{X}$ and yielded the metamodel $\tilde{\boldsymbol{\xi}}_{\boldsymbol{X_i}}$ considering the metamodel uncertainty. In summary, Table 4 and Figure 6 show the individual risk and the societal risk curve.

Table 4: relative individual risk based on the metamodels of all refinement steps to the last refinement step $\tilde{\boldsymbol{\xi}}_{\boldsymbol{X_3}}$.

metamodel	$\tilde{\boldsymbol{\xi}}_{\boldsymbol{X_0}}$	$\tilde{\boldsymbol{\xi}}_{\boldsymbol{X_1}}$	$\tilde{\boldsymbol{\xi}}_{\boldsymbol{X_2}}$	$\tilde{\boldsymbol{\xi}}_{\boldsymbol{X_3}}$
$R_{ind}/R_{ind}(\boldsymbol{\xi_{X_2}})$	7.91	2.36	1.09	1.00

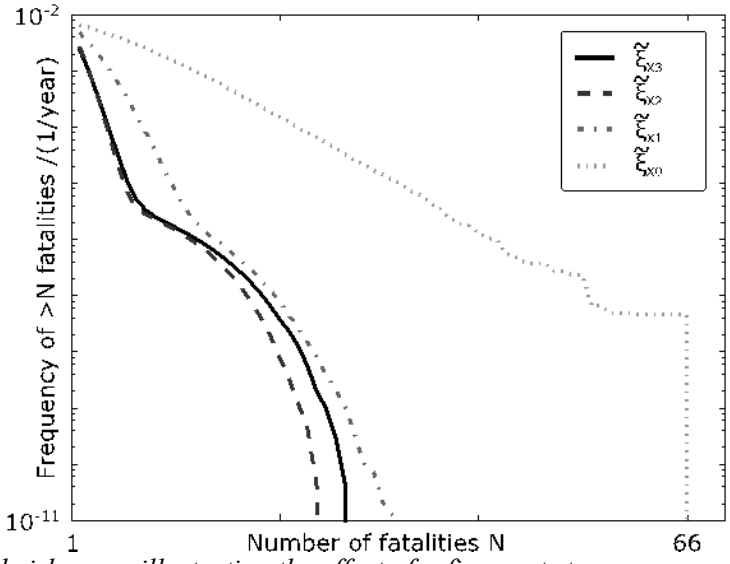

Figure 6 societal risk curve illustrating the effect of refinement steps.

We can see from Table 4 that the individual risk converges clearly to differences of less than 10% between $\tilde{\boldsymbol{\xi}}_{\boldsymbol{X_2}}$ and $\tilde{\boldsymbol{\xi}}_{\boldsymbol{X_3}}$. The societal risk curves in Figure 6 show similar behaviour. On the one hand,

$\tilde{\xi}_{X_1}$ still leads to differences to $\tilde{\xi}_{X_3}$ for small number of fatalities which can be directly linked to the metamodel. On the other hand, $\tilde{\xi}_{X_2}$ only deviates from $\tilde{\xi}_{X_3}$ for high number of fatalities in scenarios subjected to small initial frequencies. Thus, a great deal of these differences lies in the statistical uncertainties. Concluding, together with the results shown in Table 3, $\tilde{\xi}_{X_2}$ with ten fire scenarios and two times 96 evacuation scenarios ($\overline{FA}$,FA), seems to be sufficient for risk analysis.
In comparison, the methodology for risk analysis published in ISTSS 2016 [4] grounded on a metamodel with 20 fire scenarios and two times 400 evacuation scenarios. At this time, we had no option for sequential refinement in the experimental design. Thus, we simply made a very conservative guess of the required number of scenarios to get definite results which is the reason for the large discrepancy between the numbers of scenarios. From this experience we derive that the sequential refinement is very useful since it allows to get rough results quickly and then more accurate results step by step until sufficient accuracy is reached.

CONCLUSIONS

We developed a metamodel to consider complex scenarios in risk analysis including interactions between fire, tunnel users and safety measures. For this, we used the complex consequence model combining FDS [10] and FDS+Evac [11]. The metamodel consists of the projection array-based design [7] and the moving least squares method [8]. A probabilistic model based on the prediction interval [9] quantifies the metamodel uncertainty. Additionally, we implemented: first, the sequential refinement of the projection array-based design with focus on regions of the domain; and second, the combination of the experimental designs for fire and evacuation scenarios. As a result, the sequential refinement leads to convergence of the metamodel uncertainty and in risk measures with ten fire scenarios and two times 96 evacuation scenarios. In comparison to our conservative guess of the required number of scenarios published on ISTSS 2016, we state that the sequential refinement of experimental designs in general is more efficient.
The metamodel efficiently integrates complex consequence models for two reasons: first, the sequential refinement with focus on regions; and second, the combination of experimental designs. First, the sequential refinement avoids conservatively large numbers of scenarios without knowledge on the accuracy of the results.
Furthermore, we expect an efficient decrease of the metamodel uncertainty because of the local effects of sequential refinements. Second, the combination of both experimental designs reduces the number of simulations with the computationally expensive fire model. Hence, the metamodel allows considering complex scenarios with various risk indicators and interactions for risk analysis. This is an important characteristic with focus on future increasing sophistication in scenarios due to growing use of e.g. fixed fire-fighting systems or new energy carriers.
However, one open issue within our metamodel remains: the current optimisation procedure of the weighting function of the moving least squares model leads to rather global polynomial fits in contrast to our expectations. But, the optimisation procedure reduces the global metamodel uncertainty. Thus, adaptions could, on the one hand, lead to stronger local effects in the metamodel, and on the other hand, increase the metamodel uncertainty.
We finally have to emphasize that the metamodel is not limited to risk analysis but in general applicable on various experimental or modelling issues related to: (time) expensive procedures; various variables (high dimensional problems); and a global objective. To conclude, the metamodel is in particular interesting for many practical applications in fire safety demanding cost efficient solutions.

ACKNOLEDGEMENTS

The authors gratefully acknowledge the computing time granted by the JARA-HPC Vergabegremium and VSR commission on the supercomputer JURECA at Forschungszentrum Jülich.

REFERENCES

1. World Road Association (PIARC), "Current practice for risk evaluation for road tunnels", Paris, 2012.

2. Santner, T. J., Williams, B. J., and Notz, W. I., *The Design and Analysis of Computer Experiments,* Springer, New York, 2003.
3. ILF Consulting Engineers, "Erweiterung und Vertiefung des österr. Tunnelmodells - TuRisMo 2-Arbeitsbericht zum Arbeitsausschuss Tunnel-Sicherheit", 31.03.2015, Linz, 2015.
4. Berchtold, F., Thöns, S., Knaust, C., and Rogge, A., "Risk analysis in road tunnels - Most important risk indicators", *Proceedings of the Seventh International Symposium on Tunnel Safety and Security (ISTSS),* Montreal, Canada, 16-18.03.2016.
5. Myers, R. H. and Montgomery, D. C., *Response surface methodology,* J. Wiley, New York, 2002.
6. Shields, M. D., Teferra, K., Hapij, A., and Daddazio, R. P., "Refined Stratified Sampling for efficient Monte Carlo based uncertainty quantification", *Reliability Engineering & System Safety***, 142,** 310–325, 2015.
7. Loeppky, J. L., Moore, L. M., and Williams, B. J., "Projection array based designs for computer experiments", *Journal of Statistical Planning and Inference***, 142,** 1493–1505, 2012.
8. Lancaster, P. and Salkauskas, K., "Surfaces Generated by Moving Least Squares Methods", *Mathematics of Computation***, 37,** 141, 1981.
9. Kim, C. and Choi, K. K., "Reliability-Based Design Optimization Using Response Surface Method With Prediction Interval Estimation", *Journal of Mechanical Design***, 130,** 121401:1-121401:12, 2008.
10. National Institute of Standards and Technology (NIST), "Fire Dynamics Simulator (Version 6.3.1)-User's Guide", NIST Special Publication 1019, Gaithersburg, Maryland, USA, 2016.
11. Korhonen, T. and Hostikka, S., "Fire Dynamics Simulator with Evacuation: FDS+Evac 2.2.1-Technical Reference and User's Guide", 2009.
12. Berchtold, F., Thöns, S., Knaust, C., and Rogge, A., "Review of road tunnel risk assessment - common aspects?", *Proceedings of the Sixth International Symposium on Tunnel Safety and Security (ISTSS)*, 669–670, Marseille, France, 12-14.03.2014.
13. International Organization for Standardization (ISO), ISO 16732-1: Fire safety engineering - Fire risk assessment - Part 1: general, 1st ed., 13.220.01 (16732-1), 2012.
14. Ingason, H. and Lönnermark, A., "Heat release rates from heavy goods vehicle trailer fires in tunnels", *Fire Safety Journal***, 40,** 646–668, 2005.
15. Centre d'Études des Tunnels (CETU), "Guide to Road Tunnel Safety Documentation-Booklet 4: Specific Hazard Investigations", Bron (France), 2003.
16. Lönnermark, A. and Ingason, H., "Recent achievements regarding heat release and temperatures during fires in tunnels", *Proceedings of the Safety in Infrastructure,* Budapest, 2004.
17. Kinateder, M., Pauli, P., Müller, M., Krieger, J., Heimbecher, F., Rönnau, I., Bergerhausen, U., Vollmann, G., Vogt, P., and Mühlberger, A., "Human behaviour in severe tunnel accidents: Effects of information and behavioural training", *Transportation Research Part F: Traffic Psychology and Behaviour***, 17,** 20–32, 2013.
18. Nilsson, D., Johansson, M., and Frantzich, H., "Evacuation experiment in a road tunnel: A study of human behaviour and technical installations", *Fire Safety Journal***, 44,** 458–468, 2009.
19. World Road Association (PIARC), "Fire and Smoke Control in Road Tunnels", 05.05.B, Paris, 1999.
20. Bundesanstalt für Straßenwesen (BASt), *Bewertung der Sicherheit von Strassentunneln,* Wirtschaftsverlag NW, Verlag für Neue Wissenschaft GmbH, Bremerhaven, 2009.
21. Ingason, H., "Design fire curves for tunnels", *Fire Safety Journal***, 44,** 259–265, 2009.
22. McKay, M. D., Beckman, R. J., and Conover, W. J., "A Comparison of Three Methods for Selecting Values of Input Variables in the Analysis of Output from a Computer Code", *Technometrics***, 21,** 239–245, 1979.
23. Most, T. and Bucher, C., "New concepts for moving least squares: An interpolating non-singular weighting function and weighted nodal least squares", *Engineering Analysis with Boundary Elements***, 32,** 461–470, 2008.